JOURNAL OF CATALYSIS 141, 71–81 (1993)

Reactant-Promoted Reaction Mechanism for Water–Gas Shift Reaction on Rh-Doped CeO_2

TAKAFUMI SHIDO[1] AND YASUHIRO IWASAWA[2]

Department of Chemistry, Faculty of Science, The University of Tokyo, Hongo Bunkyo-ku, Tokyo 113, Japan

Received July 7, 1992; revised December 9, 1992

Reactant-promoted reaction mechanism for catalytic water–gas shift reaction (WGSR) on Rh-doped CeO_2, including the activation of intermediate by a reactant, has been investigated by FT-IR. The intermediate of WGSR on Rh/CeO_2 is bidentate formate produced from CO and terminal (on-top) surface OH groups on Ce ions: 65% of the surface formates decomposed to –OH + CO (backward decomposition) and only 35% of them decomposed to H_2 + CO_2 (forward decomposition) in vacuum. In the coexistence of second-adsorbed water molecules, almost 100% of the formate decomposed to H_2 + CO_2. Besides the direct change of decomposition selectivity, the rate constant of the forward decomposition and the activation energy were surprisingly affected by water coadsorption. The rate constant increased one hundred times and the activation energy decreased from 55.6 to 33.3 kJ mol^{-1}. The rate-determining step for catalytic WGSR on Rh/CeO_2 is the decomposition of the bidentate formate to H_2 and unidentate carbonate. The desorption of CO_2 by the decomposition of unidentate carbonate was also promoted by H_2O coexistence. The phenomena observed on Rh/CeO_2 are entirely different from those on pure CeO_2 and similar to the case of ZnO surface. The reactant-promoted reaction mechanism for WGSR is illustrated.

INTRODUCTION

We have reported a reactant-promoted reaction mechanism for the catalytic water–gas shift reaction (WGSR: H_2O + CO → H_2 + CO_2) on MgO (*1*), ZnO (*2*), and CeO_2 (*3*) as the genesis of surface catalysis. The reaction intermediate of the WGSR is formate (bidentate or bridge) produced from CO and surface OH groups (formed by the dissociation of first-adsorbed H_2O molecules). In the reactant-promoted mechanism, even if the formate intermediate is never converted to the WGSR product, H_2 and CO_2 in vacuum, or even if a minority of the formate can be transformed to H_2 and CO_2 in vacuum, 100% or a majority of the formates are converted to H_2 and CO_2 in the coexistence of second H_2O molecules adsorbed adjacently to the formate intermediate. The rate of the formate decomposition is promoted by the presence of a second water molecule and the selectivity of the formate decomposition (forward/backward) is also increased by the water coexistence. Thus, under catalytic reaction conditions of these surfaces H_2O and CO are converted to H_2 and CO_2. Among the three oxides, CeO_2 was contrasted to two other oxides (*3*). The surface formate on CeO_2 was stabilized by water coexistence, rather than being promoted. Both forward and backward decompositions of the formate were suppressed. The selectivity to the WGSR products increased as a result of the greater suppression of the backward decomposition of formate by water coexistence. The absence of a reactant-promoted effect on CeO_2 may be due to the intrinsic nature of CeO_2 or due to the stable structure of the CeO_2 surface. We have tried to modify the properties of the CeO_2 surface by doping Rh to CeO_2.

[1] Present address: Catalysis Research Center, Hokkaido University, Sapporo 060, Japan.

[2] To whom correspondence should be addressed.

0021-9517/93 $5.00

Rh is an important element of automobile exhaust catalysts (*4*). CeO_2-supported Rh catalysts have been investigated in various catalytic reactions such as CO oxidation (*5*) and syngas reaction (*6*). Hence it is important to investigate the nature of CeO_2 support in a Rh/CeO_2 system.

In this paper, (1) we produced surface formates on Rh-doped CeO_2 by the reaction of CO and the OH groups of CeO_2 surface, which were monitored and characterized by FT-IR (ν_{as}(OCO), ν_s(OCO), ν(OH)); (2) investigated the behavior of the surface formates in the presence of coadsorbed water to examine the coadsorbate effect in the rate and selectivity of the formate by FT-IR, TPD, and isotope tracer techniques; and (3) presented the reactant-promoted reaction mechanism for WGSR on Rh/CeO_2 as a basic aspect of catalysis. These are also discussed in relation to the previous observations on MgO (*1*), ZnO (*2*), and CeO_2 (*3*).

EXPERIMENTAL

CeO_2 was obtained by the calcination of $Ce(OH)_3$ at 673 K for 4 h. $Ce(OH)_3$ was obtained by precipitation of $Ce(NO_3)_3$ (Soekawa Co. Ltd., 99%) with NH_3(aq). Rh-doped CeO_2 catalysts were prepared by the usual impregnation method using an aqueous solution of $Rh(NO_3)_3$ followed by drying at 383 K and calcination in air at 673 K for 2 h. The loading of Rh was always of 0.2 wt%.

IR, TPD, and kinetic experiments are described in the previous papers (*1*, *2*). Briefly, ca. 30 mg of the sample was pressed into a self-supported disc 20 mm in diameter. The disc was placed in the holder of an IR cell which was combined with a closed circulating system, and oxidized with O_2 at 773 K for 1 h, followed by evacuation at 773 K for 1 h; then the sample was cooled down under vacuum and was reduced with H_2 at 623 K for 30 min, followed by evacuation at the same temperature. A liquid-nitrogen trap was used to trap H_2O or CO_2 during the oxidation and reduction procedure. The reduced sample was exposed to water vapor (ca. 1 kPa) for 30 min at 473 K, followed by evacuation at 623 K for 1 h. To achieve the introduction of OD groups to the CeO_2 surface, the sample was reduced by D_2 and exposed to D_2O vapor, where the procedure is the same as that in the case of H_2 and H_2O. IR spectra were measured at 300 K or reaction temperatures with a resolution of 2 or 4 cm^{-1}.

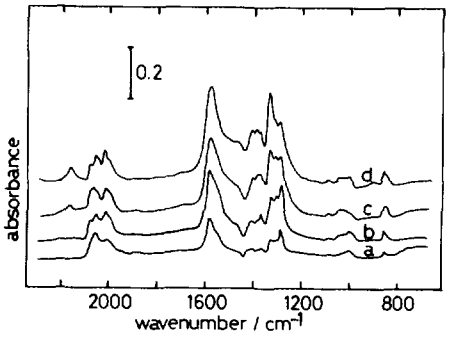

FIG. 1. IR spectra after CO adsorption on Rh/CeO_2 with OD groups. The sample was exposed to 4.0 kPa of CO for 30 min at (a) 303 K, (b) 373 K, (c) 443 K, and (d) 513 K.

TPD studies were performed in a closed circulating system. Gaseous species and desorbed species were analyzed by gas chromatography or mass spectrometry (MS). About 0.2 g of Rh-doped CeO_2 was used for TPD experiments.

The catalytic WGSR and each reaction were carried out in a closed circulating system equipped with a gas chromatograph and a mass spectrometer. The decomposition kinetics of the formates was also conducted in a closed circulating system by IR or MS.

RESULTS

1. IR Spectra

Figure 1 shows IR spectra of adsorbed CO species on Rh/CeO_2. OD groups were introduced to the CeO_2 surface by reduction with D_2 followed by exposure to D_2O, as described in the experimental section. When the sample was exposed to CO at 303

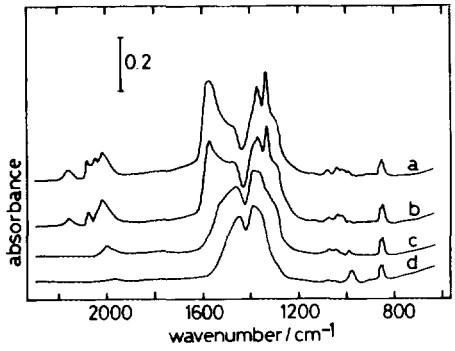

FIG. 2. IR spectra after evacuation at different temperatures following CO (4.0 kPa) adsorption on Rh/CeO_2 with OD groups at 373 K for 2 h; evacuation temperatures (a) 373 K, (b) 473 K, (c) 573 K, and (d) 673 K.

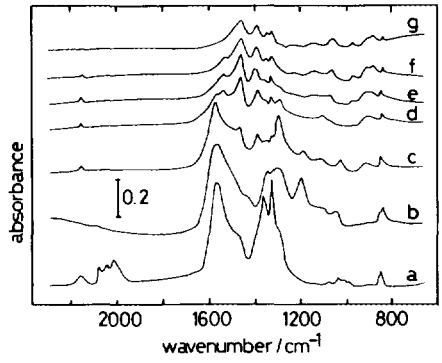

FIG. 3. IR spectra after CO adsorption on Rh/CeO_2 with OD groups at 373 K followed by evacuation at the same temperature (a) and after the sample (a) was exposed to 0.67 kPa of D_2O at 303 K (b), followed by evacuation at (c) 303 K, (d) 373 K, (e) 423 K, (f) 473 K, and (g) 523 K.

K, the IR bands appeared at 2050, 2000, 1575, 1540, 1333, and 1290 cm^{-1}. When the sample was exposed to CO at the higher temperatures (373, 443, and 513 K) another peak appeared at 2154 cm^{-1} and the intensity of the peaks at 1575, 1333, and 1290 cm^{-1} increased.

When the sample exposed to CO at 373 K was evacuated at 373, 473, 573, and 673 K, the intensity of the bands at 2154, 1575, and 1333 cm^{-1} decreased, and that of the bands at 1460 and 1390 cm^{-1} increased, as shown in Fig. 2. The IR bands in 2050–2000 cm^{-1} region also decreased in intensity with a slight red shift.

The sample which was exposed to CO and evacuated at 373 K was further exposed to 0.67 kPa of D_2O at 303 K (see Fig. 3). Then the sample was evacuated at different temperatures. When the sample was exposed to D_2O vapor, the bands at 2000–2050 cm^{-1} disappeared and the peaks at 1290–1500 cm^{-1} shifted. When the sample was evacuated at 303 K, those bands returned to the previous position. Further, when the sample was evacuated at 423 K, the intense bands at 1570 and 1290 cm^{-1} almost diminished. The bands at {1575, 1290 cm^{-1}} behaved in a manner similar to each other upon heating. The bands at {1460, 1390, and 1060 cm^{-1}} and at {2154, 1540, and 1333 cm^{-1}} also changed in intensity similar to each other (see Figs. 2 and 3). Table 1 summarizes the IR bands of surface species on Rh/CeO_2. The assignment is discussed hereinafter.

Figure 4 shows IR spectra of surface OD groups on Rh/CeO_2. Two sharp bands were observed at 2713 and 2682 cm^{-1}, and two broad bands were observed at 2580 and 2530 cm^{-1}. When the sample was exposed to CO at 373 K, the intensity of only the 2713-cm^{-1} peak decreased. When the sample was evacuated at 513 K, the intensity of both IR bands at 2713 and 2682 cm^{-1} decreased, and a new band at 2694 cm^{-1} appeared.

TABLE 1

Absorption Bands of Adsorbed Species on Rh/CeO_2

Adsorbate	Wavenumber of IR bands (in cm^{-1})
Bidentate formate[a]	ν(CH), 2861(2154); ν_{as}(OCO), 1555(1540); ν_s(OCO), 1358(1333)
Unidentate carbonate	ν_{as}(OCO), 1460; ν_s(OCO), 1390; ν(CO), 1060
Bidentate carbonate	ν(C=O), 1575; ν_{as}(OCO), 1290; ν_s(OCO), 1032

[a] The former value and the latter value in parentheses respresent the wavenumber of IR bands corresponding to HCOO and DCOO, respectively.

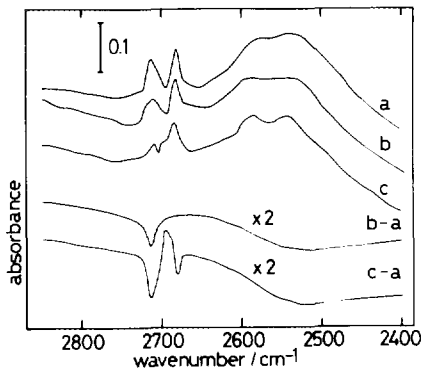

FIG. 4. IR spectra of surface OD groups on Rh/CeO_2 (a) and after the exposure to CO at 373 K (b) followed by evacuation at 513 K (c).

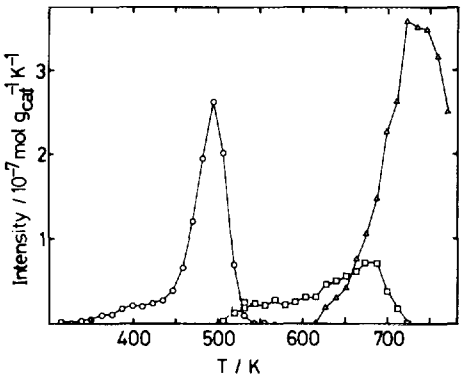

FIG. 6. TPD spectra of adsorbed species on Rh/CeO_2. The sample was exposed to CO at 373 K, followed by evacuation at 303 K. Heating rate is 3.0 K min^{-1}: (○) CO, (□) H_2, and (△) CO_2.

2. *Temperature-Programmed Desorption Experiments*

Figure 5 shows the amount of water produced in H_2 reduction as a function of reduction temperature. The oxidized Rh/CeO_2 was exposed to 4.0 kPa of hydrogen for 20 min at given temperatures. The temperature was increased successively. The integrated amounts of H_2O produced at each temperature are shown in Fig. 5. The reduction of the sample began at 473 K. The reducing rate was almost constant up to 673 K and increased above 673 K.

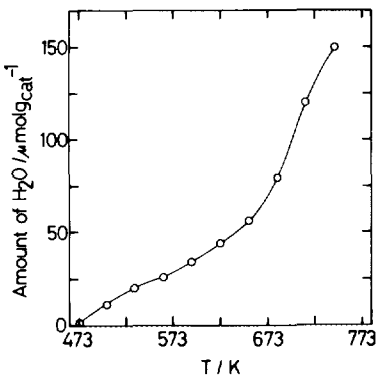

FIG. 5. Amounts of water produced as a function of reduction temperature. The oxidized Rh/CeO_2 was exposed to 4.0 kPa of hydrogen at given temperatures for 20 min.

Figure 6 shows the TPD spectrum after CO adsorption on Rh/CeO_2. The reduced Rh/CeO_2 was exposed to CO at 373 K for 30 min, followed by evacuation at 303 K. The heating rate was 3.0 K min^{-1}. A desorption peak of CO appeared at 490 K, and hydrogen began to desorb at 513 K with a peak at 650–700 K. CO_2 desorption was observed above 610 K, showing a peak at 720 K. The desorption amounts of CO and hydrogen were 13.3 and 7.8 $\mu mol\ g_{cat}^{-1}$, respectively.

Figure 7 shows the TPD spectrum from

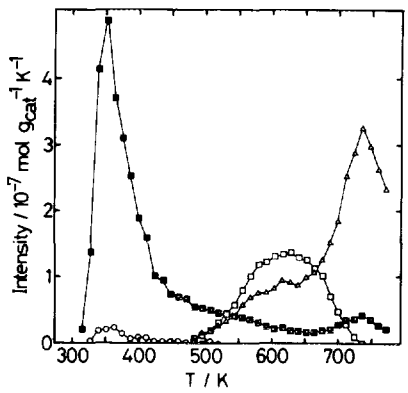

FIG. 7. TPD spectra of adsorbed species on Rh/CeO_2 in the presence of coadsorbed water. The sample was exposed to CO at 373 K, followed by evacuation at 303 K, and then exposed to 0.67 kPa of D_2O followed by evacuation at 303 K. Heating rate is 3.0 K min^{-1}: (○) CO, (■) H_2O, (□) H_2, and (△) CO_2.

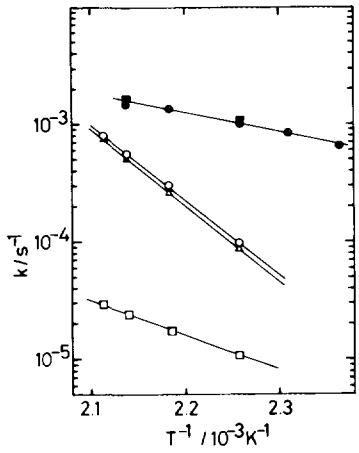

FIG. 8. Arrhenius plots for the decomposition of surface formates: (○) $k_+ + k_-$, (□) k_+, and (△) k_- in the absence of water; (●) $k_- + k$ and (■) k_- in the presence of water.

adsorbed formate and water. The reduced Rh/CeO_2 was exposed to CO at 303 K, followed by evacuation at 303 K. Then the sample was exposed to water vapor at 303 K, followed by evacuation at the same temperature. Desorption peaks of water, hydrogen, and CO_2 appeared at 350, 610, and 730 K, respectively. Desorption amounts of water, hydrogen, and CO_2 were 41.6, 19.5, and 37.1 μmol g_{cat}^{-1}, respectively; 1.2 μmol g_{cat}^{-1} of CO desorbed with a peak at 360 K. When water coadsorbed, the desorption peak of hydrogen shifted to lower temperature by 50 K, and the amount of hydrogen produced became 2.5 times as large as that produced from surface formates without coadsorbed water. Further, the desorption peak of CO at 490 K disappeared by water coadsorption.

3. *Kinetic Studies*

Figure 8 shows the Arrhenius plots of the decomposition of surface formates on Rh/CeO_2. The formates were formed by admitting 4.0 kPa of CO to the Rh/CeO_2 reduced with $H_2(D_2)$ at 623 K and exposed to $H_2O(D_2O)$ at 473 K as described in the Experimental section. The total rate constant ($k_+ + k_-$) for the decomposition was obtained from the decrease rate of the intensity of ν(CD) of formates at constant temperatures. Each rate constant, k_+ and k_- for the forward and backward decomposition, respectively, was obtained from the decrease of the desorbed amounts of H_2 and CO, respectively, detected by MS. Logarithms of the IR peak intensity or the MS signal intensity were plotted as a function of the reaction time, and the reaction rate constants were calculated by the least-squares fit of the plots. Most of the surface formates decomposed to OD + CO in vacuum. The value of k_+ was more than 10 times smaller than that of k_-. The activation energy for k_- and k_- were 55.6 and 122 kJ mol^{-1}, respectively. The value of $k_+ + k_-$ that was obtained by IR spectra agreed with the sum of k_+ and k_-. When water vapor coexisted, $k_+ + k_-$ became about 10 times larger than that without water. Almost all of the formates decomposed to $CO_2 + D_2$, and the backward decomposition was not observed in the presence of water. The value of k_+ agreed with that of $k_+ + k_-$, and the activation energy was determined to be 33.3 kJ mol^{-1}. The value of k_+ in the presence of water was 100 times larger than that of k_+ *in vacuo*, and the activation energy decreased by 20 kJ mol^{-1}.

Figure 9 shows k_+ as a function of adsorbed amount of water. k_+ linearly increased with an increased of the adsorbed amount of undissociated water.

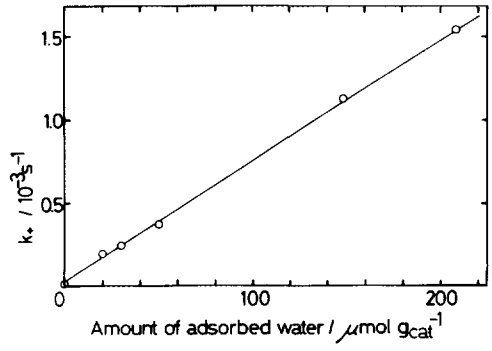

FIG. 9. Values of k_+ at 443 K as a function of amounts of adsorbed water.

TABLE 2

Rate Constants of the Forward Decomposition of Bidentate Formates (DCOO) on Rh/CeO_2 in the Presence of Various Coadsorbed Molecules[a]

Molecules	k_+ (s^{-1})
None	1.1×10^{-5}
H_2O	1.12×10^{-3}
CH_3OH	1.58×10^{-3}
Pyridine	5.8×10^{-4}
THF	2.0×10^{-4}

[a] T = 443 K, 0.67 kPa of gases were introduced.

The values of k_+ measured in the presence of various coadsorbed molecules are shown in Table 2. When water or methanol coexisted on Rh/CeO_2 surface, k_+ became 100 times larger than that *in vacuo*. When pyridine or THF (tetrahydrofuran) coexisted, k_+ became 20–50 times as large as that *in vacuo*. Surface formates were activated more by water and methanol.

Table 3 shows k_+ in various isotope combinations of hydrogen in formate and water molecules. The rate constant for the forward decomposition of formates was mainly affected by the hydrogen isotope in the formate and little by the hydrogen isotope in the water molecule. The value of k_+ for HCOO decomposition is ca. 1.4 times larger than that of DCOO.

TABLE 3

Rate Constants of the Forward Decomposition of Bidentate Formates on Rh/CeO_2 at 443 K in Various Combinations of Hydrogen Isotope

Combination	k_+ (10^{-3} s^{-1})
HCOO + H_2O	1.49
HCOO + D_2O	1.47
DCOO + H_2O	1.12
DCOO + D_2O	1.05

Table 4 compares the observed rate of the catalytic WGSR and the calculated value from k_+ and the adsorbed amount (M) of formate in reaction conditions. The adsorbed amount of the formate under reaction conditions was estimated as follows. After the measurement of the reaction rate, the gas phase was evacuated and the catalyst was heated to 773 K. The amount of the formate was estimated from the sum of the desorbed amount of $H_2(D_2)$ and CO during the heating.

DISCUSSION

1. Assignment of Adsorbed Species on Rh/CeO_2

As shown in Fig. 3, the IR peaks at 2154, 1540, and 1333 cm^{-1} behaved in a similar way upon heating, suggesting that those peaks originate from the same species. The frequency of these bands shifted by isotope exchange (D → H) of surface hydroxyl groups on Rh/CeO_2; 2100–2200, 1500–1600, and 1300–1400 cm^{-1} are the region of ν(CD), ν_{as}(OCO), and ν_s(OCO), respectively, characteristic of formates. The structure of formate can be estimated by the difference ($\Delta\nu$) of wavenumber between ν_{as}(OCO) and ν_s(OCO) (*1*, *7*). When $\Delta\nu$ is larger than that of a free ion ($\Delta\nu$ of a free ion is ca. 220 cm^{-1}), the formate is unidentate formate, and when the value of $\Delta\nu$ is the same as or smaller than that for a free ion, the formate is bridge formate or bidentate formate, respectively. The structures and ν_{as}(OCO) and ν_s(OCO) of several metal formate complexes have been reported. The value of $\Delta\nu$ for the bridge-type formate are in the range ca. 220–280 cm^{-1}, and those of unidentate- and bidentate-type formates are larger than 300 cm^{-1} and around 200 cm^{-1}, respectively. The value of $\Delta\nu$ for the surface formate on Rh/CeO_2 is 197 cm^{-1} as shown in Table 1. Hence, the surface formate produced on Rh/CeO_2 is assigned to be bidentate formate.

The $\Delta\nu$'s of the bidentate formate on MgO, ZnO, and CeO_2 have been observed to be 222, 201, and 189 cm^{-1}, respectively

TABLE 4

Comparison between the Observed Rate of WGSR on Rh/CeO_2 and the Calculated Value from k_+ and Adsorbed Amount of Formate with Reaction Conditions[a]

Reactant	T (K)	k_+ (10^{-3} s^{-1})	M (μmol g_{cat}^{-1})	$k_+ \times M^b$	r^c
H_2O + CO	443	1.49	6.8	10	11
H_2O + CO	468	2.44	5.4	13	15
D_2O + CO	443	1.05	6.0	6.3	5.9
D_2O + CO	468	1.64	5.0	8.2	8.0

[a] $P(H_2O)$ or $P(D_2O)$ = 0.67 kPa and $P(CO)$ = 4.0 kPa.
[b] nmol g_{cat}^{-1} s^{-1}.
[c] Rate of WGSR in nmol g_{cat}^{-1} s^{-1}.

(*1–3*). The ν_{as}(OCO) and ν_s(OCO) for CeO_2 were 1547 (1540: D-exchange) and 1358(1338) cm^{-1} (*3*), which are almost the same as those for Rh/CeO_2 (1555(1540) and 1358(1333) cm^{-1}) in Table 1. The WGSR did not proceed on Rh/SiO_2 in the temperature range 420–520 K. These results demonstrate that the bidentate formate is not produced on Rh metal or Rh ion, but produced on Ce ion of CeO_2.

The IR bands at {1460 and 1390 cm^{-1}} and {1575, 1290, and 1032 cm^{-1}} are attributed to the same species, respectively, because of the similar behavior in Fig. 3. These bands did not shift by the isotope exchange of hydrogen of surface hydroxyls, suggesting that these species do not contain hydrogen atoms. Hence these IR bands may be attributed to adsorbed CO and/or CO_2 species such as carbonate or carboxylate. There are many IR spectra of carbonate and carboxylate on various oxide surfaces (*8*). As for CeO_2, the IR bands at 1454, 1348, 1062, and 854 cm^{-1} have been assigned to unidentate carbonate, and the bands at 1562, 1286, 1028, and 854 cm^{-1} and 1510, 1310 cm^{-1} have been attributed to bidentate carbonate and carboxylate, respectively (*9, 10*). Hence, the IR bands at 1460, 1390, and 1060 cm^{-1} are assigned to unidentate carbonate, and the bands at 1575, 1290, and 1032 cm^{-1} are attributed to bidentate carbonate.

The IR bands at 2054, 2017 cm^{-1} were observed when the sample was exposed to CO in Fig. 1. Upon heating, more bands appeared in Fig. 1. These bands disappeared by evacuation at 573–673 K. The frequencies are similar to these of ν(CO) for CO adsorption on Rh metal particles.

The IR bands of the surface OD groups on Rh/CeO_2 appeared at 2713, 2680, 2582, and 2530 cm^{-1}, whose wavenumbers are almost the same as those of OD groups on CeO_2. The IR bands at 2713, 2682, 2580, and 2530 cm^{-1} have been assigned to terminal, bridge, and two hollow-site OD groups, respectively (*3*). The peak intensity of the bridge OD groups on Rh/CeO_2 is larger than that on 623-K reduced CeO_2. This fact suggests that the surface density of oxygen atoms on Rh/CeO_2 is smaller than that on CeO_2. In other words, there may be more oxygen defects on Rh/CeO_2 than on CeO_2. The bridge OD groups would be formed by the interaction with two Ce ions having a defect at the inbetween sites.

2. *Properties of Surface Species on Rh/CeO_2*

Compared with the surface formate on CeO_2, the surface formate on Rh/CeO_2 has two characteristic properties. One is that the decomposition temperature of the formate on Rh/CeO_2 (450 K) is lower than that of the formate on CeO_2 (600 K). The surface formates on both Rh/CeO_2 and CeO_2 surface are present as bidentate formates at the decomposition temperature. The activation energy of the decoposition of the formate on

Rh/CeO_2 (e.g., 55.6 kJ mol^{-1} for k_+) is also lower than that on CeO_2 (207 kJ mol^{-1} for k_+). Another characteristic nature is that only bidentate formate was produced on Rh/CeO_2 surface when the sample was exposed to CO, whereas bridge formate was produced on CeO_2 by CO exposure at room temperature and the bridge formate was converted to bidentate formate above 500 K. Thus, bidentate formates are more easily produced and decomposed on Rh/CeO_2 than on CeO_2. Since the formates are located on CeO_2 surfaces in both catalysts, the difference may be caused by the difference in the degree of coordination unsaturation of Ce ions between the two catalysts.

As shown in Fig. 4, the terminal OD groups at 2713 cm^{-1} reacted with CO to form bidentate formates. The reaction of the terminal hydroxyl groups with CO is a common feature with MgO, ZnO, and CeO_2 (*1–3*). When the surface bidentate formate decomposed, the IR band of bridge OD groups at 2682 cm^{-1} decreased as shown in Fig. 4. In the forward decomposition to form H_2 and CO_2, it is necessary for the formate hydrogen to combine with an adjacent H atom. Thus, the forward decomposition of the bidentate formate is suggested to proceed by the reaction of the formate with the adjacent bridge hydroxyl group. The feature is similar to that observed with ZnO (*2*). By evacuation at 513 K in Fig. 4, the on-top OD groups at 2713 cm^{-1} decreased while a new peak at 2694 cm^{-1} appeared. This was also observed with the CeO_2 catalyst, where the oxygen atom of on-top OD groups was suggested to interact with the adjacent Ce ion (*3*).

The intensity of the bidentate carbonate peak on Rh/CeO_2 is much larger than that on CeO_2. To produce bidentate carbonates, at least two coordination sites on Ce ion are necessary, which is compatible with the higher degree of coordination unsaturation on Ce ions of Rh/CeO_2. From the comparison of the IR spectra with the TPD spectra the bidentate carbonate is decomposed to CO at 360 K in the presence of water in Figs. 4 and 7.

The reduction of the sample with H_2 at 623 K removes the surface oxygen to create the coordinatively unsaturation sites on Ce ions. Oxygen migrates from CeO_2 bulk to surface, however, and the most oxygen deficiency at the pure CeO_2 surface is suppressed. The lower coordination unsaturation of the surface was achieved by Rh addition (0.2 wt%). The Rh/CeO_2 surface is homogeneous in a meaning that only bidentate formate was observed. If this is not the case, two kinds of CeO_2 surfaces affected and unaffected by Rh would exist and hence both bidentate and bridge formates would have been formed.

3. Interaction between Surface Formate and Water

The decomposition of the surface bidentate formate on Rh/CeO_2 was markedly affected by the presence of water; 63% of the formates decomposed to CO + –OH (backward) and 37% of them decomposed to H_2 + CO_2(ad) (forward) in vacuum. When 0.67 kPa of water vapor coexisted, almost 100% of the surface formates decomposed toward the forward direction and the backward decomposition was not observed. Besides the enhancement of the decomposition selectivity, the rate constant of decomposition increased in the presence of water; the value of k_+ became 100 times as large as that without water. The activation energy of the forward decomposition decreased from 55.6 kJ mol^{-1} (without water) to 33.3 kJ mol^{-1} (with water). These results demonstrate that the change of the selectivity (forward/backward) is not caused by an equilibrium shift but ascribed to the change of reaction path/reaction mechanism. Thus the water molecule (reactant of the WGSR) promoted the forward decomposition of the formate intermediate and suppressed the backward decomposition of the intermediate. The k_+ increased with an increase of the adsorbed amount of undissociated water in the range of the adsorbed amount 0–220 $\mu mol\ g_{cat}^{-1}$, which demonstrates direct and local effects of

adsorbed water molecules on the formate decomposition.

This promoting effect was also observed when methanol, THF, pyridine were introduced (Table 2). Thus the driving force of this interaction may be electron donation from the added molecules to the Ce ion on which the formate exists. However, the promotion by H_2O and CH_3OH was larger than that by pyridine and THF. The former molecules can interact with Ce–O pairs at the surface in an electron donor–acceptor pair mode, but the latter molecule interact with Ce ions alone. Electron transfer from the oxygen atom of a Ce–O pair to the OH hydrogen of H_2O or CH_3OH through hydrogen bonding (the positively charged H atom ($H^{\delta+}$) of H_2O withdraws electrons of the O ion of CeO_2 surface) decreases the diameter of surface oxygen ion and the electron donation from the oxygen lone pair electrons to the Ce ion becomes stronger.

On the contrary, the surface formates on the CeO_2 catalyst were stabilized by water coexistence as previously reported (*3*), where the rate constant ($k_+ + k_-$) of the formate decomposition decreased to 1/18 in the presence of H_2O. The backward decomposition of the formate was more suppressed and as a result, the forward decomposition was preferable in the coexistence of water. This kind of stabilization of surface formate by coadsorbed water has been observed on MgO (*1*) but not observed on ZnO (*3*). The kinetic data on Rh/CeO_2 are entirely different from those for CeO_2. On Rh/CeO_2 the reaction rate increased and the activation energy decreased in the coexistence of H_2O, as already mentioned. The difference between Rh/CeO_2 and CeO_2 was also observed with hydrogen isotope effects.

The isotope effects were observed with the hydrogen atom of formate and not observed with the hydrogen atom of the water molecule, as shown in Table 3. Hence, the rate determining step of the formate decomposition on Rh/CeO_2 is suggested to be dissociation of the CH bond of the bidentate formate. The result is similar to that observed on ZnO (*2*). In contrast, the isotope effects on CeO_2 were observed with the hydrogen atoms of both formate and water, where the activation of both the C–H bond of the formate and the O–H bond of the adjacent bridge OH groups in the transition state is necessary. The local structure and arrangement of the Ce–O reaction sites appear to be different between the Rh/CeO_2 and CeO_2 surfaces, which must be caused by the difference of the degree of surface reduction. It is suggested that charge rearrangement and local restructuring on the Ce–O reaction sites as a result of adding Rh cause the activation of the CH bond of the formate intermediate involving a tilting to the adjacent bridge OH in the transition state decreased in the next section, which leads to the much lower activation energy and the switchover of the reaction path (selectivity) for the WGSR.

4. Reaction Mechanism of Surface Formate

The reaction rates obtained from the rate constants of the forward decomposition of the surface bidentate formate agreed with the catalytic WGSR rate under various conditions in Table 4. It demonstrates that the surface bidentate formate is an intermediate of WGSR on Rh/CeO_2. The bidentate formate was converted to unidentate carbonate as shown in Figs. 2 and 3. Similar to the case of the CeO_2 surface, unidentate carbonate hardly desorbs in reaction conditions as shown in Fig. 6, but the decomposition to CO_2 was promoted by H_2O coexistence in Fig. 7. The temperature range for the decomposition of unidentate carbonate to CO_2 is wide in Fig. 7, which indicates that there are different types of unidentate carbonates on Rh/CeO_2 surface.

Scheme 1 shows the reaction mechanism of the catalytic WGSR on Rh/CeO_2. Terminal hydroxyl groups react with CO to produce bidentate formates. In vacuum, 65% of the surface formates decompose to $-OH + CO$ (backward reaction) and 35% of them decompose to $CO_2 + H_2$ (forward

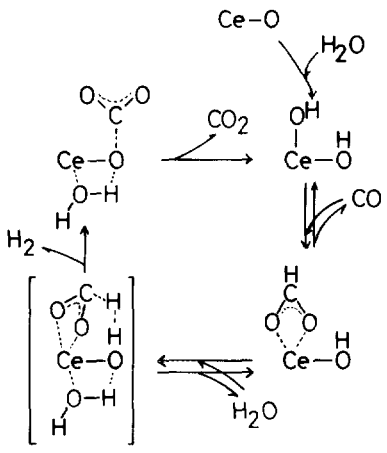

SCHEME 1. A reaction mechanism for WGSR on Rh/CeO_2.

reaction) by the reaction with bridge OH. When water coexists, 100% of the formates decompose to $H_2 + CO_2$. Scheme 1 is essentially the same as the mechanism for the WGSR on ZnO (*2*).

By addition of a small amount of Rh (0.2 wt%), the rate of WGSR increased tremendously, and the value of k_+ was promoted about 100 times by the coexistence of H_2O molecules. The frequencies of the IR peaks of adsorbed species such as formate, carbonate and hydroxyl groups on Rh/CeO_2 were almost the same as those on CeO_2. It means that the electronic states of Ce–O pairs on CeO_2 and Rh/CeO_2 are not different. Rather, the local structure/the surface morphology around the reaction site on CeO_2 surface may be changed by reduction with H_2 in the presence of the supported Rh particles.

Electron donation from H_2O to the Ce ion to which the bidentate formate is coordinated is an essential factor to promote the forward decomposition of the surface formate. The hydrogen bonding of hydrogen atom ($H^{\delta+}$) of H_2O to withdraw electrons from the O ion of a Ce–O pair also contributes to the promoting effect. The desorption of the adsorbed CO_2 (unidentate carbonate) formed from the formate is also promoted dissociative adsorption of water.

CONCLUSION

(1) The catalytic WGSR proceeds on Ce–O pair sites of Rh/CeO_2, not on Rh metallic particles. Rh/SiO_2 was inactive under similar reaction conditions.

(2) On-top (terminal) OH groups on Ce ions react with CO to form bidentate formates.

(3) The bidentate formate is decomposed to H_2 and unidentate carbonate.

(4) The rate constants of bidentate formate decomposition were determined by FT-IR in various reaction conditions. The WGSR rates are reproduced by the calculated rates $k_+ \times M$, where k_+ and M represent the rate constant of the forward decomposition of bidentate formate and the adsorbed amount of the formate, respectively, suggesting that the rate-determining step of WGSR on Rh/CeO_2 is the decomposition of bidentate formate.

(5) The rate constant of the forward decomposition of bidentate increased 100 times by the coexistence of H_2O molecules.

(6) The activation energy of the formate decomposition decreased from 55.6 kJ mol^{-1} in vacuum to 33.3 kJ mol^{-1} in the presence of H_2O.

(7) Water molecules also promote the desorption of the carbonate as CO_2.

(8) The rate constant (k_+) increased linearly with an increase of the amount of undissociated water adsorbed (second-adsorbed molecules).

(9) Electron donor–acceptor interaction between Ce–O pairs and water molecules is suggested to be an important factor for reactant-promoted catalysis.

(10) Reactant-promoted mechanism for the WGSR is observed with Rh/CeO_2, in contrast to CeO_2 where the formate was stabilized by water coexistence.

REFERENCES

1. Shido, T., Asakura, K., and Iwasawa, Y., *J. Catal.* **122**, 55 (1990).

2. Shido, T., and Iwasawa, Y., *J. Catal.* **129,** 343 (1991).
3. Shido, T., and Iwasawa, Y., *J. Catal.* **136,** 493 (1992).
4. Wei, J., *Adv. Catal.* **24,** 57 (1975).
5. Su, E. C., Montreuil, C. N., and Rothschild, W. G., *Appl. Catal.* **17,** (1985).
6. Kiennemann, A., Breault, R., and Hindermann, J-P., *J. Chem. Soc. Faraday Trans. 1* **83,** 2119 (1987).
7. Nakamoto, K., "Infrared and Raman Spectra of Inorganic and Coordination Compounds," 3rd ed. Wiley–Interscience, New York, 1987.
8. Little, L. H., "Infrared Spectra of Adsorbed Species." Academic Press, New York, 1966.
9. Li, C., Sakata, Y., Arai, T., Domen, K., Maruya, K., and Onishi, T., *J. Chem. Soc. Faraday Trans. 1* **85,** 929 (1989).
10. Jin, T., Zhou, Y., Mains, G. J., and White, J. M., *J. Phys. Chem.* **91,** 5931 (1987).